Available online at www.sciencedirect.com
ScienceDirect
Journal of Photochemistry and Photobiology B: Biology 86 (2007) 199–206
Journal of Photochemistry and Photobiology B:Biology
www.elsevier.com/locate/jphotobiol

Activity of Subtilisin Carlsberg in macromolecular crowding

Ajay Kumar Shaw, Samir Kumar Pal *

Unit for Nano Science and Technology, Department of Chemical, Biological and Macromolecular Sciences, S. N. Bose National Centre for Basic Sciences, Block JD, Sector III, Salt Lake, Kolkata 700 098, India

Received 28 July 2006; received in revised form 6 October 2006; accepted 10 October 2006
Available online 15 November 2006

Abstract

Enzymatic activity of a proteolytic enzyme Subtilisin Carlsberg (SC) in anionic sodium dodecyl sulfate (SDS) micellar medium has been explored and found to be retarded compared to that in bulk buffer. Circular dichroism (CD) study reveals that SDS, which is a potential protein denaturant, has an insignificant denaturation effect on SC. The structural integrity of the protein offers an opportunity to study the functionality of the enzyme SC in a macromolecular crowding of micelles. Dynamic light scattering (DLS) data indicates no sandwich-like micelle–SC complex formation ruling out the possibility of interaction of the enzyme with the hydrophobic core of the micelle. However, steady state and time resolved emission studies on specific and nonspecific fluorescent probes indicate the proximity effect at the surface of the enzyme due to macromolecular crowding of the micelles. The agreement of retarded enzymatic activity in the micellar crowd with a theoretical model ascribed to the facts that substrates are compartmentalized in the micelles and enzyme interacts with the micelle through stern layer.

Keywords: Subtilisin Carlsberg; SDS micelle; Enzyme kinetics; Time resolved absorption; Circular dichroism; Picosecond resolved fluorescence anisotropy

1. Introduction

Enzymatic activity of cytosolic enzymes *in vitro* condition where solution contains very low concentration of protein, substrate and salt, shows different behavior relative to that *in vivo* condition. In the living cell a significant fraction of the total volume is ''crowded'' by several other macromolecular solutes [1–3]. Crowding can also affect equilibrium of an enzymatic reaction by destabilizing either reactant or products, such that the most favored state excludes the least volume to the other macromolecular species present in the solution [2]. Therefore, an accurate evaluation of the physiological role of a particular reaction characterized *in vitro* is done by considering the possible influence of crowding and/or confinement upon the reaction. The catalytic properties of an enzyme in microheterogeneous micellar medium [4] and organic solvents [5–8] can be helpful to the understanding of the catalytic mechanism in the living cell.

Till date there has been enumerable studies on enzymatic activities involving all possible enzymes in an attempt to explain the influence of environment around the biocatalyst and the structure of enzymes on the enzymatic activities [9–15]. Catalytic activities of enzymes have also been carried out in micellar environment [3,4,16–20], which is very often considered as a mimic of physiological environment for biomolecules. It has been found on the basis of previous studies on the enzymatic activity of α-chymotrypsin that the activity of the enzyme is 7 times retarded upon complexation with cetyl trimethyl ammonium bromide (CTAB) micelle [18], while it is retarded by two orders of magnitude when encapsulated inside AOT reverse micelle [17]. Sodium dodecyl sulfate (SDS), an anionic surfactant is known to bind strongly to most proteins and cause surfactant induced unfolding [21–23]. Serious investigation has led to the emergence of three useful models [23] for the structure of SDS-protein complex – (i) ''Necklace and bead model'', (ii) ''rod-like'' prolate ellipsoidal surfactant

* Corresponding author. Fax: +91 33 2335 3477.
E-mail address: skpal@bose.res.in (S.K. Pal).

1011-1344/$ - see front matter © 2006 Elsevier B.V. All rights reserved.
doi:10.1016/j.jphotobiol.2006.10.001

aggregate with a semi-minor axis around 18 Å, and (iii) a "flexible capped helical cylindrical micelle" with proteins wrapping around the micelle.

Here we report activity of an enzyme *Subtilisin Carlsberg* (SC) in an aqueous micellar solution. The anionic SDS micelle of diameter 3.3 nm [24] is considered as a biomimetic system. The enzyme SC (EC: 3.4.21.62) from *Bacillus licheniformis* containing a single polypeptide chain of 274 amino acid residues with two Ca^{2+} ion binding sites [25] is in a class of serine endopeptidase. The diameter of SC (4.2 nm) is also comparable [26] to that of the SDS micelle. We observed that the rate of enzymatic reaction of SC on various substrates is retarded and depends heavily on the micellar concentration in the host solution. In order to understand the dependence of the enzymatic activity on micellar concentration, we fit our experimental results to a theoretical model [27] proposed recently for enzymatic activity in aqueous micellar solution. To follow the environmental change at a particular site of the enzyme SC upon interaction with the micelle, intrinsic single tryptophan residue (Trp113) is used as fluorescent probe. The overall environmental change around SC in the micellar solution is followed from the steady state and time resolved fluorescence spectroscopy of a covalently attached dansyl-probe (nonspecifically labeled) at the surface of the enzyme. Circular dichroism (CD) and dynamic light scattering (DLS) studies reveal the overall structural changes of the enzyme SC upon complexation with SDS micelle. Our studies reveal that the retardation of enzymatic activity of SC in the micellar crowd is *not* solely due to structural perturbation of the protein; rather the affinity of the substrate and enzyme towards the micelle is the determining factor for the retardation.

2. Materials and methods

Subtilisin Carlsberg (EC 3.4.21.62), Ala-Ala-Phe 7-amido-4-methyl coumarin (AAF-AMC), *N*–CBZ-Gly-Gly-Leu *p*-nitroanilide (CBZ–GGL–pNA), sodium monophosphate and sodium diphosphate were procured from Sigma chemicals (St. Louis, USA). Sodium dodecyl sulfate (SDS) and dansyl chloride (DC) were purchased from Fluka (St. Louis, USA) and Molecular Probes (Carlsbad, USA) respectively. All the samples were used as received without further purification. Distilled water from Millipore system was used. All the sample solutions were prepared in 0.1 M phosphate buffer. The covalent attachment of DC to SC (adduct formation) was achieved following the procedure from Molecular Probes [28]. Briefly, DC was dissolved in a small amount of dimethyl formamide and then injected into the 0.1 M sodium bicarbonate solution (pH 8.3) of SC. The reaction was terminated by adding a small amount of freshly prepared hydroxylamine (1.5 M, pH 8.5) after incubating it for 1 h at 4–8 °C with continuous stirring. The solution was then dialyzed exhaustively against phosphate buffer (0.1 M) to separate adducts (DC–SC) from any unreacted DC and its hydrolysed product. It should be noted that DC–SC complexes (SC:DC = 1:2) are quantitatively formed because of covalent synthesis.

Steady-state absorption and emission were measured with Shimadzu Model UV-2450 spectrophotometer and Jobin Yvon Model Fluoromax-3 fluorimeter respectively. The circular dichroism study was done using Jasco 810 spectropolarimeter using a quartz cell of path-length 10 mm. The secondary structural data of the CD spectra were analyzed using CDSSTR program of CDPro software [29,30]. CDSSTR program is a modification of VARSLC (variable Selection), which uses all possible combinations of a fixed number of proteins in the reference set. VARSLC, or Variable Selection, from Johnson et al. [31] fits a random subset of eight basis spectra using the variable selection method first described by Mosteller and Tukey [32]. The resulting fits are analyzed using four criteria: (i) The sum of the secondary structures is close to unity, (ii) No fraction of the secondary structure be less than 0.03, (iii) The reconstituted CD spectrum should fit the original spectrum with only a small error, (iv) The fraction of alpha-helix should be similar to that obtained using all the proteins as the basis set. The subset that fits these criteria best is used as the basis set.

Dynamic light scattering (DLS) measurement were done with Nano-S Malvern instruments (UK), employing a 4 mW He–Ne laser ($\lambda = 632.8$ nm) and equipped with a thermostatted sample chamber. All measurements were taken at 173° scattering angle at 298 K. The scattering intensity data are processed using the instrumental software to obtain the hydrodynamic diameter (d_H) and the size distribution of the scatterer in each sample. The instrument measures the time dependent fluctuation in intensity of light scattered from the particles in solution at a fixed scattering angle. Hydrodynamic diameters (d_H) of the particles are estimated from the intensity autocorrelation function of the time-dependent fluctuation in intensity. d_H is defined as

$$d_H = kT/3\pi\eta D \quad (1)$$

where k is the Boltzmann constant; T, the absolute temperature; η, the viscosity and D, the translational diffusion coefficient. In a typical size distribution graph from the DLS measurement X-axis shows a distribution of size classes in nm, while the Y-axis shows the relative intensity of the scattered light. This is therefore known as an intensity distribution graph.

Catalytic measurements of SC were made using the substrates AAF-AMC and CBZ–GGL–pNA. The extinction coefficients used for determining the concentrations of AAF-AMC and CBZ–GGL–pNA in buffer (pH = 7.0) are 16 $mM^{-1}\,cm^{-1}$ (at 325 nm) and 14 $mM^{-1}\,cm^{-1}$ (at 315 nm) respectively [15]. The extinction coefficients of the products formed are 7.6 $mM^{-1}\,cm^{-1}$ (for AMC at 370 nm) and 8.8 $mM^{-1}\,cm^{-1}$ (for pNA at 410 nm). The extinction coefficient for determination of concentration of SC in buffer is 23.46 $mM^{-1}\,cm^{-1}$ at 278 nm. For the enzymatic kinetics experiment the enzyme concentration

was maintained at 15 μM while that of substrate was maintained at 150 μM. The rate of formation of product was monitored using the change in absorbance of the product with time.

All the fluorescence transients were recorded using picosecond-resolved time correlated single photon counting (TCSPC) technique at 54.7° (magic angle) with respect to polarization axis of the excitation beam. The TCSPC setup was from Edinburgh instruments, UK. In order to excite dansyl probe and AMC chromophore (substrate and product) an excitation laser source of wavelength 375 nm (instrument response function (IRF) ~ 98 ps) was used. Excitation of the tryptophan residue of the enzyme SC was made by a LED source of wavelength 299 nm (IRF ~460 ps). For temporal fluorescence anisotropy measurements emission polarization was adjusted to be parallel or perpendicular to that of the excitation and define anisotropy as $r(t) = [I_{para} - G \cdot I_{perp}]/[I_{para} + 2 \cdot G \cdot I_{perp}]$. The G factor was determined to be 1.1.

3. Results and discussion

Fig. 1a shows the schematic diagram of the enzyme Subtilisin Carlsberg (PDB code: 1SCD) [26] depicting the positions of amino acid residues (Asp32, His64 and Ser221) of the catalytic triad at the active site [33]. The single tryptophan residue (Trp113) and one of the dansyl-binding sites (Lys136) at the surface of SC are also indicated. Fig. 1b shows the CD spectra of SC in buffer, 1, 40 and 100 mM SDS. The fitted data reveals helicity of 34.8% (buffer), 32.2% (1 mM SDS), 34.6% (40 mM SDS) and 31.3% (100 mM SDS). The α-helical content is consistent with that of the native SC (34%) in the crystalline state [34], indicating insignificant structural perturbation of the enzyme upon interaction with SDS micelle. It has been shown earlier that SDS monomers below their critical micellar concentration (CMC; 3.3 mM in buffer) are associated with other transport protein Bovine Serum Albumin (BSA) through hydrophobic interaction and denature the protein at higher SDS concentration (much above CMC) to form necklace–bead type structure in the solution [23]. Similar interaction of the SDS molecules with the enzyme SC is expected to lead to a different secondary structure of SC at higher SDS concentration than that at lower concentration of SDS. Our observation of the persistency of structural integrity of SC below and much above the CMC of SDS rules out the possibility of any specific interaction of monomeric SDS molecules with the enzyme.

Fig. 2a shows the rate of formation of AMC-product upon enzymatic activity of SC on AAF-AMC in buffer and in SDS solutions of different concentrations. The velocities of AMC-product formation in buffer, 1mM SDS and 40 mM SDS are 41.5×10^{-3}, 18.1×10^{-3} and 0.2×10^{-3} μM s^{-1} respectively. It is clear that the activity of the enzyme is retarded by 2.3 and 244 times in 1 mM and 40 mM SDS respectively compared to that in buffer solution. We also checked the activity of the enzyme on a

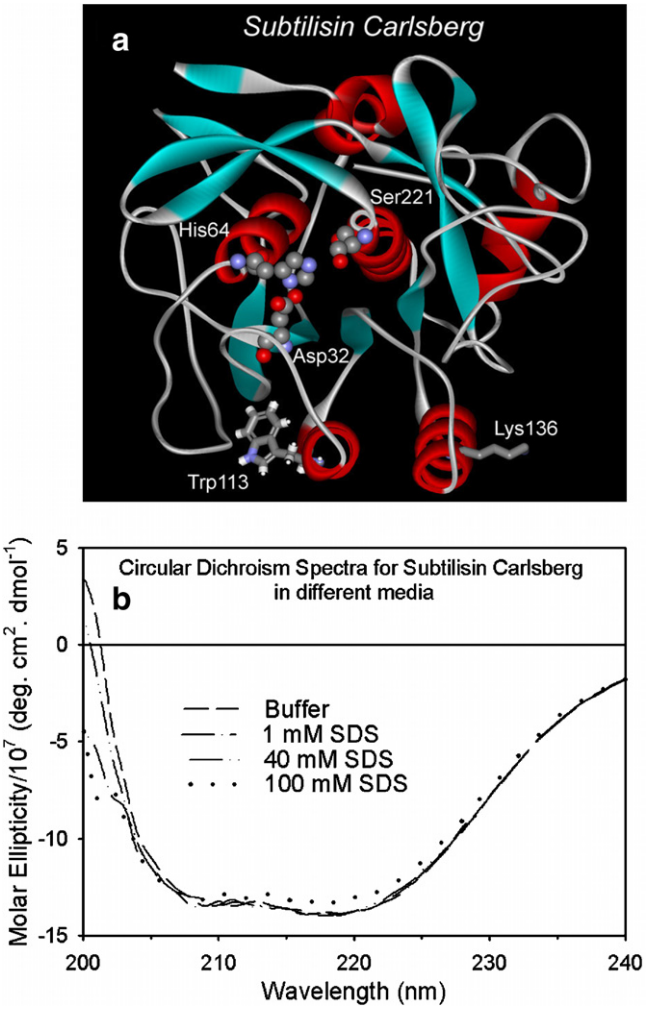

Fig. 1. (a) High resolution X-ray structure of *Subtilisin Carlsberg* (PDB code: 1SCD). (b) The CD spectra of SC in buffer and SDS solutions of various concentrations.

different hydrophobic (completely insoluble in water) substrate CBZ–GGL–pNA (Fig. 2b) and the activity is found to be much higher compared to the case of AAF-AMC (344.9×10^{-3} and 30.2×10^{-3} μM s^{-1} in 1 and 40 mM SDS solutions respectively). The higher enzymatic activity on CBZ–GGL–pNA could be due to much higher affinity of the substrate towards the enzyme [15]. In order to check the enzymatic activity of SC on this substrate in bulk buffer, we have measured the enzymatic reaction rate in acetonitrile-buffer (8% v/v) solution. The rate is much faster (1.551 μM s^{-1}) than that in surfactant solutions.

In order to understand the retardation of enzymatic activity in the micellar solution we measured the rates of enzymatic catalysis by SC in the surfactant solutions with various micellar concentrations and fitted the data points by simplex method using the theoretical "pseudophase" model, initially introduced for enzymes encapsulated in reverse micelles [35] and recently advanced for enzymes in aqueous micellar environments [27]. According to the model [27] the substrate can partition between three

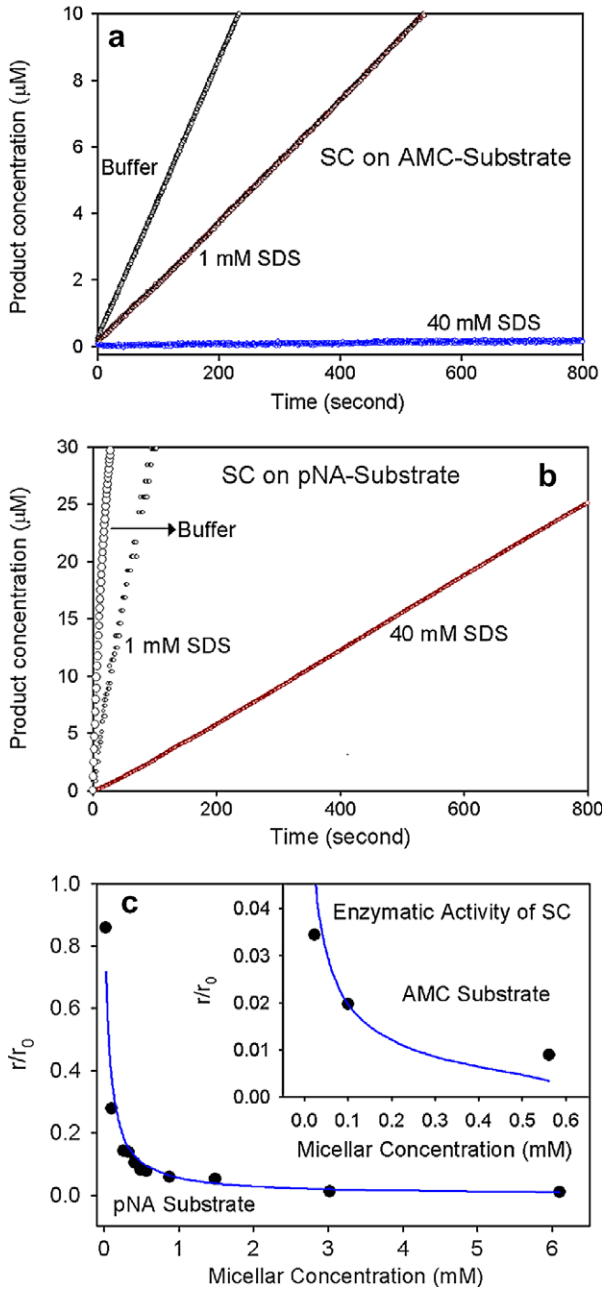

Fig. 2. Enzymatic activities of SC on various substrates: (a) AAF-AMC, (b) CBZ-GGL-pNA and (c) the relative rate of enzymatic activities of the enzyme SC on CBZ-GGL-pNA substrate. The solid line corresponds to the fitting data according to the pseudophase model (see text).

pseudo-phases of the micelle, namely, free water, bound water and surfactant aggregate. Here we consider the interaction of the enzyme with the micelle through bound water (stern layer) and *not* directly with the hydrophobic part of the surfactant molecule. In the latter case structural perturbation and formation of sandwich-like micelle-enzyme complex are unavoidable. Our CD, DLS and steady-state fluorescence studies (see below) justify the assumption very well. The overall rate of substrate consumption, r, is given by [27]

$$r = \frac{k_{\mathrm{cat}}^{\mathrm{ff}} \cdot [E_{\mathrm{f}}] \cdot [S_{\mathrm{f}}]}{K_{\mathrm{m}}^{\mathrm{ff}} + [S_{\mathrm{f}}]} + \frac{k_{\mathrm{cat}}^{\mathrm{fb}} \cdot [E_{\mathrm{f}}] \cdot [S_{\mathrm{b}}]}{K_{\mathrm{m}}^{\mathrm{fb}} + [S_{\mathrm{b}}]} + \frac{k_{\mathrm{cat}}^{\mathrm{bf}} \cdot [E_{\mathrm{b}}] \cdot [S_{\mathrm{f}}]}{K_{\mathrm{m}}^{\mathrm{bf}} + [S_{\mathrm{f}}]} + \frac{k_{\mathrm{cat}}^{\mathrm{bb}} \cdot [E_{\mathrm{b}}] \cdot [S_{\mathrm{b}}]}{K_{\mathrm{m}}^{\mathrm{bb}} + [S_{\mathrm{b}}]} \quad (2)$$

where $[E]$ and $[S]$ indicate enzyme and substrate concentrations respectively. The subscripts f, b and s refer to the free water, the bound water and surfactant molecules respectively. The double superscripts refer to the pseudo-phases in which the enzyme (first superscript) and substrate (second superscript) are confined. K_{m} and k_{cat} indicate Michaelis constant and catalytic rate constant of the enzymatic reaction respectively. A thermodynamic equilibrium between the free water and the whole micellar aggregate is assumed as follows:

$$[S_{\mathrm{f}}] + [D_{\mathrm{N}}] \overset{K_{\mathrm{S}}}{\leftrightarrow} [S_{\mathrm{m}}] \quad (3)$$

where K_{S} is the association constant and $[D_{\mathrm{N}}]$ is the concentration of surfactant micellar aggregates, which can be determined from the difference between the CMC and the total concentration of surfactant in the system. Partition equilibrium between the substrate in the bound water, $[S_{\mathrm{b}}]$, and that associated with the micellized surfactant $[S_{\mathrm{s}}]$, is introduced as follows:

$$[S_{\mathrm{b}}] \overset{P_{\mathrm{bs}}}{\leftrightarrow} [S_{\mathrm{s}}] \quad (4)$$

where P_{bs} is the partition coefficient. The above conditions lead to the following relationships for the concentrations of substrate, which are able to react in the presence of micelles:

$$[S_{\mathrm{f}}] = \frac{[S_{\mathrm{t}}]}{1 + K_{\mathrm{s}} \cdot [D_N]} \quad (5)$$

$$[S_{\mathrm{b}}] = \frac{K_{\mathrm{S}} \cdot [D_{\mathrm{N}}]}{(1 + K_{\mathrm{S}} \cdot [D_{\mathrm{N}}]) \cdot (1 + P_{\mathrm{bs}})} \cdot [S_{\mathrm{t}}] \quad (6)$$

where $[S_{\mathrm{t}}]$ is the total concentration of the substrate in the solution. To describe the enzyme partition in the pseudo-phases, the following equilibrium is assumed:

$$[E_{\mathrm{f}}] + [D_{\mathrm{N}}] \overset{K_{\mathrm{E}}}{\leftrightarrow} [E_{\mathrm{b}}] \quad (7)$$

where K_{E} is the constant of association between the enzyme and micelle. We also have,

$$[E_{\mathrm{f}}] = \frac{[E_{\mathrm{t}}]}{1 + K_{\mathrm{E}} \cdot [D_{\mathrm{N}}]} \quad (8)$$

$$[E_{\mathrm{b}}] = \frac{K_{\mathrm{E}} \cdot [D_{\mathrm{N}}] \cdot [E_{\mathrm{t}}]}{1 + K_{\mathrm{E}} \cdot [D_{\mathrm{N}}]} \quad (9)$$

In principle, on applying Eqs. (5), (6), (8) and (9) in Eq. (2) one can obtain the overall enzymatic reaction rate (r). In order to disregard the change in the rate due to interaction of surfactant monomer with the enzyme, a relative rate (r/r_0) with various micellar concentrations can be considered, where r_0 is the reaction rate at the critical micellar concentration (CMC). However, in our studies we considered r_0 at 1 mM SDS, which is below the CMC of the surfactant (3.3 mM) [23].

In Fig. 2c the plot of (r/r_0) refers to the relative rates of two substrates consumption. The solid line corresponds to the fitting data according to the model where the concentration of the substrate in the bound phase is negligible in comparison to that of the substrate associated with the surfactant, $[S_b] \ll [S_S]$, i.e. the substrate aggregated in the micelles is all segregated by the surfactant. The condition is attained at $P_{bs} \gg 1$ and implies that $[S_m] \approx [S_s]$. This assumption determines that $[S_b] \approx 0$, independently of the equilibrium constant of the substrate–micelle association, K_s. As a consequence, the second and fourth terms in Eq. (2) can be neglected. Thus, the final form of rate of catalysis is as follows:

$$r = \frac{[E_t][S_t]}{1 + K_E[D_N]} \left\{ \frac{\eta_{ff}}{(1 + K_S[D_N]) + [S_t]/K_m^{ff}} + \frac{[D_N]K_E\eta_{bf}}{(1 + K_S[D_N]) + [S_t]/K_m^{bf}} \right\} \quad (10)$$

In our studies it is found that the enzymatic activity monotonically decreases with the increase in micellar concentration (Fig. 2c). Here we maintained the enzyme and substrate concentrations to be 0.015 mM and 0.150 mM respectively. The initial velocity (rate) of substrate consumption was measured upto a surfactant concentration of 400 mM for CBZ–GGL–pNA. From the simulation (Fig. 2c, solid line) the parameter η_{ff} is found to be five orders of magnitude higher for CBZ–GGL–pNA substrate compared to that for the AAF-AMC which is consistent with the previous report [15]. Since the enzymatic activity of SC with the substrate AAF-AMC falls much more steeply with the surfactant concentration (inset of Fig. 2c) compared to that with CBZ–GGL–pNA, only few data points were obtained. Evaluation of six parameters from the numerical fitting of only modest number of experimental points is not reliable. However, the agreement of the trend of the experimental data points with that of the model fitting is clear from the inset of Fig. 2c.

DLS experiments (Fig. 3a) reveal hydrodynamic diameter of the micelle (40 mM SDS) and SC (native) to be 4.35 nm of 5.10 nm respectively. Considering typical thickness of the hydration layer to be ~0.5 nm, our experimental observations are in good agreement with actual diameters of the micelle and the native protein, which are reported to be 3.3 and 4.2 nm respectively [24,26]. The peaks due to particles with higher hydrodynamic diameter (100 nm and larger) in surfactant solutions could be due to the presence of higher micellar aggregates in the solutions. Note that in the intensity distribution graph, the area of the peak for the larger particles will appear at least 10^6 times larger than the peak for the smaller particles. This is because large particles scatter much more light than small particles, as the intensity of scattering of a particle is proportional to the sixth power of its diameter (Rayleigh's approximation). Thus the number densities of larger particles in our solutions are negligibly small. The hydrodynamic diameter of SC in presence of the micelle is found

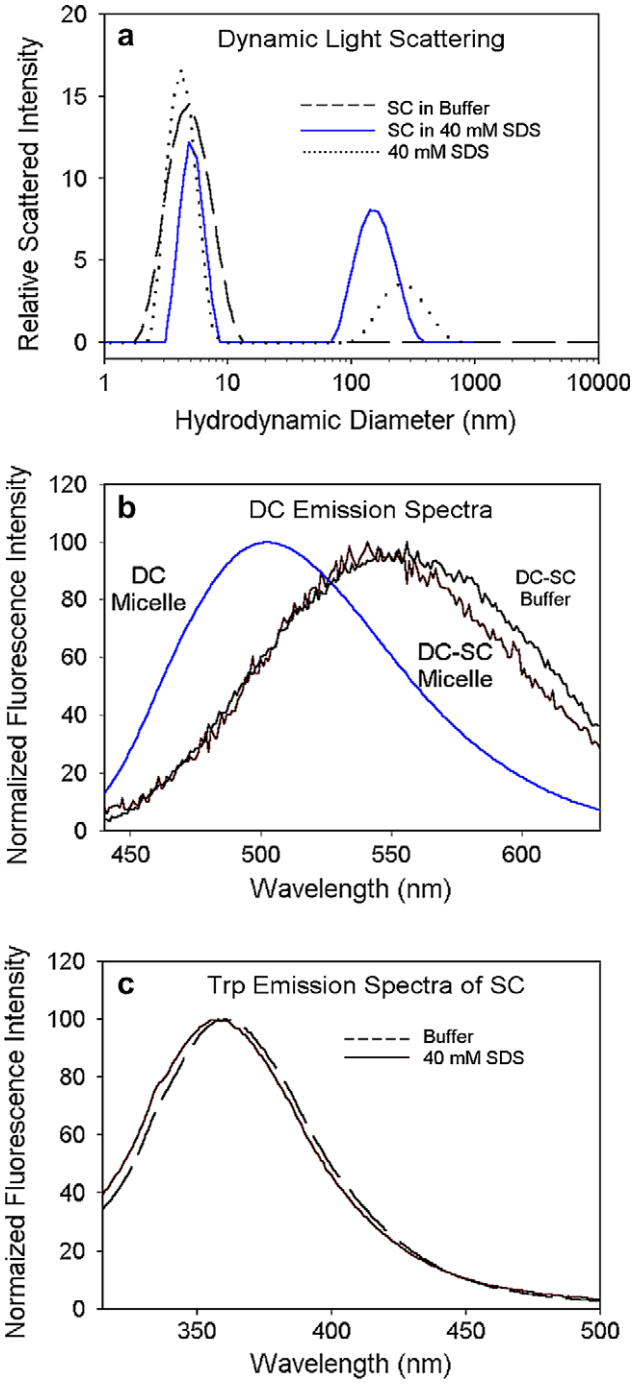

Fig. 3. (a) The dynamic light scattering spectra of SC in buffer (dash), SC in 40 mM SDS (solid) and 40 mM SDS micelle (dot). (b) The emission spectra of dansyl probe in DC–micelle complex, DC–SC–micelle complex and DC–SC complex in buffer. (c) The emission spectra of Trp113 residue of SC in buffer and 40 mM SDS solutions.

to be 5.20 nm revealing the intactness of the globular structure of the enzyme in the surfactant solution. The intactness of the secondary structure as evident from CD studies along with the preservation of globular structure indicates the retention of tertiary structure of the enzyme in the surfactant solution. The observation also rules out the possibility of formation of sandwich-like complex

where the resulting diameter is expected to be ~10 nm. However, the interaction of the enzyme with the micelle is clearly evident from steady state fluorescence spectra of the DC–SC (Fig. 3b). The emission maximum of DC–SC in buffer at 555 nm shifts to 541 nm in 40 mM SDS indicating that DC bound to SC finds itself close to the surface of SDS micelle, namely, stern layer. The inclusion of the enzyme into the micelle can also be ruled out from the steady-state emission studies as the emission maximum of DC–SC–micelle complex (541 nm) is considerably red shifted compared to that of DC embedded in SDS micelle (502 nm).

Fig. 4a and b show the temporal fluorescence anisotropy ($r(t)$) decays of AAF-AMC in buffer and 40 mM SDS respectively. Fig. 4c shows temporal evolution of $r(t)$ of the AMC chromophore (product) in 40 mM SDS. The rotational correlation time (ϕ) of AAF-AMC in 40 mM SDS (202 ps (15%), 1334 ps (56%) with a much longer time constant which does not decay in our experimental time window) is much slower than that in bulk buffer solution (222 ps). This considerable slowing down of rotational time constant of AAF-AMC in 40 mM SDS medium indicates strong affinity of the substrate to the micelle. However, AMC-product in 40 mM SDS micelle reveals two ϕ values; 184 ps (64%) and 1800 ps (15%) with a much longer time constant, which does not decay in our experimental time window. The existence of faster time constant (64%) in the fluorescence anisotropy of the AMC product reflects lesser micellar affinity compared to that of the substrate. The higher affinity of the substrate for the micelle indicates the segregation possibility of the substrate into the hydrophobic core of the micelle. The anisotropy data of pNA-substrate and product are quite complicated due to its intricate internal dynamics, which is under investigation.

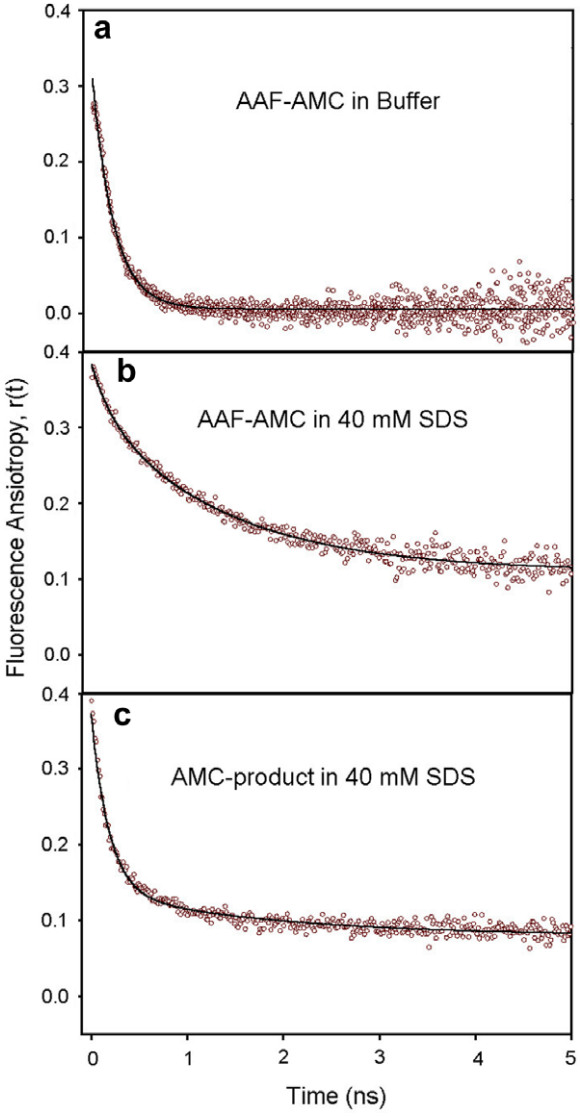

Fig. 4. The temporal fluorescence anisotropy decay curve of: (a) AAF-AMC substrate in buffer, (b) AAF-AMC substrate in 40 mM SDS and (c) AMC-product in 40 mM SDS.

In order to investigate the nature of complexation of SC with the micelle, we have also studied the emission properties of single tryptophan (Trp113) residue of the enzyme (Fig. 3c). The emission maximum of Trp113 in buffer (λ_{max} = 360 nm) shifts to 358 and 356 nm in 40 mM and 100 mM SDS micellar solutions respectively. The minute change in the emission maximum of Trp113 compared to that of the enzyme-bound DC might indicate involvement of specific site/sites (excluding Trp113) of SC for the interaction with SDS micelle. The temporal anisotropy decay of Trp113 in buffer (time constant 496 ps (70%) with a much longer time component, which does not decay in our experimental time window) is comparable to that of SC–SDS complex (451 ps (68%) with a much longer time component, which does not decay in our experimental time window) as shown in Fig. 5a and b. The observation excludes any significant interaction of SC with SDS micelle through the Trp113 site. Another possibility of the negligible change in the anisotropy decay of Trp113 could be due to the buried nature of Trp113 in SC. However, our steady state fluorescence studies indicate that the emission maximum of Trp113 has no shift compared to that of the free tryptophan in bulk buffer reflecting significant exposure of the Trp113 residue of the SC towards bulk buffer. The conclusion is further supported by a recent MD simulation study [36], which confirmed that Trp113 residue of SC is edge exposed and the contribution to the Stokes shift from the bulk water is much larger (70%) than that from the protein environment (polar/charged residues). Thus the less change in the fluorescence anisotropy of the probe Trp113 upon interaction with SDS micelle cannot be due to the buried nature of the probe in the enzyme SC. The fluorescence anisotropy decay of the nonspecific label DC which essentially probes all the surface sites of the enzyme in buffer (Fig. 5c) shows time constants of 3970 ps (47%) and 50 000 ps (53%). The faster and slower time constants can be attributed to the local tumbling of the probe and global rotational motion of the labeled protein respectively. In 40 mM SDS (Fig. 5d) solution the DC labeled enzyme shows three distinct time constants in the fluorescence

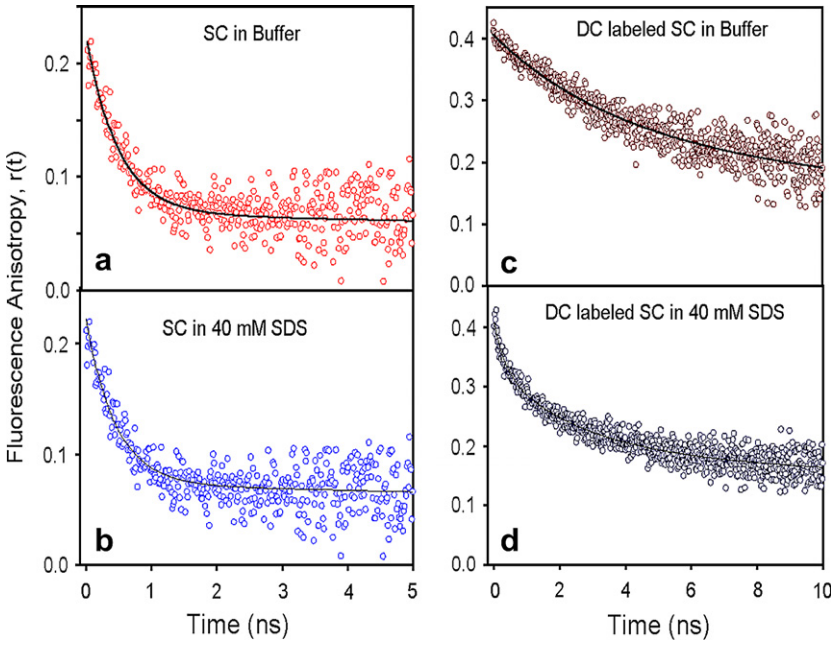

Fig. 5. The temporal fluorescence anisotropy decay curve of Trp113 of SC in (a) buffer and (b) 40 mM SDS while that of DC–SC complex in (c) buffer and (d) 40 mM SDS.

anisotropy decay; 334 ps (19%), 2555 ps (36%) and 71156 ps (45%). The presence of the faster time constant (334 ps, 19%) in the DC–SC–micelle complex in contrast to the native DC–SC may indicate a minute local structural perturbation reflecting reorientation of a particular dansyl chromophore in the perturbed site of the enzyme. However, the global rotational motion of the enzyme in the micellar crowding is indeed slowed down considerably.

4. Conclusion

From the present study it is found that SC retains its structural integrity in SDS solution, which is a potential protein denaturant. From DLS experiments no evidence of sandwich-like SC–SDS complex formation is found indicating that SC does not encroach into the hydrophobic surfactant core of SDS micelle to form an elongated structure. Nonspecifically and specifically labeled fluorescence probes have been employed in order to investigate the nature of the complexation. The steady-state and time resolved fluorescence anisotropy of a fluorescent tag DC at the nonspecific sites of the enzyme, which essentially probes polarity and geometrical restriction on the surface of the enzyme SC show evidence of micellar crowding in the vicinity of the enzyme. However, the moderate change in the emission properties and temporal anisotropy dynamics of the intrinsic fluorophore Trp113 at a specific site of the enzyme reflects participation of specific site/sites (excluding Trp113) of the enzyme for the interaction with SDS micelle. Our studies on the enzyme kinetics of native-like SC in the micellar solution support a model where the interaction of SC with the micelle through its stern layer is assumed. The model also assumes that the surfactant core of the micelle segregates the substrates in the micellar solution. Our anisotropy studies on AAF-AMC substrate in the micellar solution are consistent with the segregation picture. The reported experimental observation on the enzymatic activity of SC, with structural integrity retained (from CD studies) in a macromolecular crowding, would be useful in the understanding of the functionality of enzymes under physiological condition.

5. Abbreviations

SC	Subtilisin Carlsberg
AAF-AMC	Ala-Ala-Phe 7-amido-4-methyl coumarin
CBZ-GGL-pNA	N-CBZ-Gly-Gly-Leu *p*-nitroanilide
SDS	sodium dodecyl sulfate
CD	circular dichroism
DLS	dynamic light scattering
DC	dansyl chloride
Trp	tryptophan
IRF	instrument response function
LED	light emitting diode

Acknowledgement

AKS thanks UGC for fellowship. We thank DST for financial grant (SR/FTP/PS-05/2004).

References

[1] S.B. Zimmerman, A.P. Minton, Macromolecular Crowding: biochemical, biophysical and physiological consequences, Annu. Rev. Biophys. Biomol. Struct. 22 (1993) 27–75.

[2] B.V.D. Berg, R. Wain, C.M. Dobson, R.J. Ellis, Macromolecular crowding perturbs protein refolding kinetics: implications for folding inside the cell, EMBO J. 19 (2000) 3870–3875.
[3] A.P. Minton, The influence of macromolecular crowding and macromolecular confinement on biological reactions in physiological media, J. Biol. Chem. 276 (2001) 10577–10580.
[4] M.S. Celej, M.G. D'Adrea, P.T. Campana, G.D. Fidelio, M.L. Bianconi, Superactivity and conformational changes on a-chymotrypsin upon interfacial binding to cationic micelles, Biochem. J. 378 (2004) 1059–1066.
[5] K. Griebenow, A.M. Klibanov, On protein denaturation in aqueous-organic mixtures but not in pure organic solvents, J. Am. Chem. Soc. 118 (1996) 11695–11700.
[6] R. Affleck, C.A. Haynes, D.S. Clark, Solvent Dielectric Effects on Protein Dynamics, Proc. Natl. Acad. Sci. USA 89 (1992) 5167–5170.
[7] K. Griebenow, M. Vidal, C. Baez, A.M. Santos, G. Barletta, Nativelike Enzyme Properties Are Important for Optimum Activity in Neat Organic Solvents, J. Am. Chem. Soc. 123 (2001) 5380–5381.
[8] S.G. Martinez, E. Alvira, L.V. Cordero, A. Ferrer, I. Montanes-Clemente, G. Barletta, High Initial Activity but Low Storage Stability Observed for Several Preparations of Subtilisin Carslberg Suspended in Organic Solvents, Biotechnol. Prog. 18 (2002) 1462–1466.
[9] O.G. Berg, M.H. Gelb, M.D. Tsai, M.K. Jain, Interfacial enzymology: The secreted phospholipase A2-paradigm, Chem. Rev. 101 (2001) 2613–2653.
[10] J.L. Schmitke, L.J. Stern, A.M. Klibanov, Organic Solvent Binding to Crystalline Subtilisin1in Mostly Aqueous Media and in the Neat Solvents, Biochem. Biophys. Res. Commun. 248 (1998) 273–277.
[11] T. Ke, C.R. Wescott, A.M. Klibanov, Prediction of the Solvent Dependence of Enzymatic Prochiral Selectivity by Means of Structure-Based Thermodynamic Calculations, J. Am. Chem. Soc. 118 (1996) 3366–3374.
[12] K. Xu, pH Control of the Catalytic Activity of Cross-Linked Enzyme Crystals in Organic Solvents, J. Am. Chem. Soc. 118 (1996) 9815–9819.
[13] Y.L. Khmelnitsky, S.H. Welch, D. Clark, S.J.S. Dordick, Salts dramatically enhance activity of enzymes suspended in organic solvents, J. Am. Chem. Soc. 116 (1994) 2647–2648.
[14] R.K. Eppler, R.L.S. Komor, J. Huynh, J.S. Dordick, J.A. Reimer, D. Clark, Water dynamics and salt-activation of enzymes in Organic media: Mechanistic implications revealed by NMR spectroscopy, Proc. Natl. Acad. Sci. USA 103 (2006) 5706–5710.
[15] J.K.A. Kamal, T. Xia, S.K. Pal, L. Zhao, A.H. Zewail, Enzyme functionality and solvation of subtilisin carlsberg: From hours to femtoseconds, Chem. Phys. Lett. 387 (2004) 209–215.
[16] A.V. Levashov, N.L. Klyachko, Micellar enzymology: methodology and technique, Russian Chem. Bull. Int. Ed. 50 (2001) 1718–1732.
[17] R. Biswas, S.K. Pal, Caging enzyme function: a-chymotrypsin in reverse micelle, Chem. Phys. Lett. 387 (2004) 221–226.
[18] R. Sarkar, M. Ghosh, A.K. Shaw, S.K. Pal, Ultrafast surface solvation dynamics and functionality of an enzyme Chymotrypsin upon interfacial binding to a cationic micelle, J. Photochem. Photobiol. B Biol. 79 (2005) 67–78.
[19] C. Grandi, R.E. Smith, P.L. Luisi, Micellar solubilization of biopolymers in organic solvents. Activity and conformation of lysozyme in isooctane reverse micelles, J. Biol. Chem. 256 (1981) 837–843.
[20] B. Steinmann, H. Jackle, P.L. Luisi, A Comparative Study of Lysozyme, Conformation in Various Reverse Micellar Systems, Biopolymers 25 (1986) 1133–1156.
[21] M.N. Jones, Surfactant interactions with biomembranes and proteins, Chem. Soc. Rev. 21 (1992) 127.
[22] C. Tanford, The Hydrophobic Effect: Formation of Micellar and Biological Membranes, Wiley Interscience, New York, 1980.
[23] N.J. Turro, X.-G. Lei, K.P. Anantapadmanabhan, M. Aronson, Spectroscopic probe analysis of protein-surfactant interactions: the BSA/SDS system, Langmuir 11 (1995) 2525–2533.
[24] P.A. Hassan, S.R. Raghavan, E.W. Kaler, Microstructural changes in SDS micelles induced by hydrotropic salt, Langmuir 18 (2002) 2543–2548.
[25] S. Lee, D.-J. Jang, Progressive rearrangement of Subtilisin Carlsberg into orderly and inflexible Conformation with Ca^{2+} Binding, Biophys. J. 81 (2001) 2972–2978.
[26] P.A. Fitzpatrick, D. Ringe, A.M. Klibanov, X-ray crystal structure of cross-linked Subtilisin Carlsberg in water vs. acetonitrile, Biochem. Biophys. Res. Commun. 198 (1994) 675–681.
[27] P. Viparelli, F. Alfani, M. Cantarella, Models for enzyme superactivity in aqueous solutions of surfactants, Biochem. J. 344 (1999) 765–773.
[28] R.P. Haugland, Handbook of Fluorescent Probes and Research Chemicals, Molecular Probes, Eugene, OR, 1996.
[29] N. Sreerama, R.W. Woody, Estimation of protein secondary structure from CD spectra: comparison of CONTIN, SELCON and CDSSTR methods with an expanded reference set, Anal. Biochem. 282 (2000) 252–260.
[30] N. Sreerama, R.W. Woody, A self-consistent method for the analysis of protein secondary structure from circular dichroism, Anal Biochem. 209 (1993) 32–44.
[31] W.C. Johnson, Analyzing protein circular dichroism spectra for accurate secondary structures, Proteins Struct. Funct. Genet. 35 (1999) 307–312.
[32] F. Mosteller, J.W. Tukey, Data Analysis and Regression, Addison-Wesley, Reading, MA, 1977.
[33] P. Castner, J.A. Wells, Dissecting the catalytic triad of serine protease, Nature 332 (1988) 564–568.
[34] J.L. Schmitke, L.J. Stern, A.M. Klibanov, The crystal structure of Subtilisin Carlsberg in anhydrous dioxane and its comparison with those in water and acetonitrile, Proc. Natl. Acad. Sci. USA 94 (1997) 4250.
[35] R. Bru, A. sanchez-ferrer, F. Garcia-Garmona, A theoretical study on the expression of enzymic activity in reverse micelles, Biochem. J. 259 (1989) 355–361.
[36] J.T. Vivian, P.R. Callis, Mechanisms of tryptophan fluorescence shifts in proteins, Biophys. J. 80 (2001) 2093–2109.